

Lessons From Non-Abelian Plasma Instabilities in Two Spatial Dimensions

Peter Arnold and Po-Shan Leang

*Department of Physics, University of Virginia,
P.O. Box 400714 Charlottesville, Virginia 22904-4714, USA*

(Dated: April, 2007)

Abstract

Plasma instabilities can play a fundamental role in quark-gluon plasma equilibration in the high energy (weak coupling) limit. Early simulations of the evolution of plasma instabilities in non-abelian gauge theory, performed in one spatial dimension, found behavior qualitatively similar to traditional QED plasmas. Later simulations of the fully three-dimensional theory found different behavior, unlike traditional QED plasmas. To shed light on the origin of this difference, we study the intermediate case of two spatial dimensions. Depending on how the “two-dimensional” theory is formulated, we can obtain either behavior.

I. INTRODUCTION AND RESULTS

It is a difficult theoretical problem to fully understand how quark-gluon plasmas come to local equilibrium in the context of heavy ion collisions. In fact, equilibration is not yet fully understood even in the formal limit of weakly-coupled quark-gluon plasmas (equivalently the limit of arbitrarily high energy collisions). By investigating the rates and interplay of individual scattering processes, Baier, Mueller, Schiff and Son [1] attempted to analyze equilibration in the weak coupling limit, producing what is known as the bottom-up scenario of quark-gluon plasma equilibration. However, interesting collective behavior in the form of plasma instabilities turns out to severely complicate the problem [2]. The relevant instabilities are known in traditional plasma physics as Weibel or filamentary instabilities [3, 4, 5]. Over the last few years, there has been a variety of work on the dynamics of plasma instabilities in the weakly-coupled limit of non-abelian gauge theory [6, 7, 8, 9, 10, 11, 12, 13, 14, 15, 16, 17]. Plasma instabilities initially grow exponentially quickly, and they create large color magnetic fields which could speed up local isotropization and thermalization of the initially non-equilibrium plasma by scattering plasma particles into random directions. To puzzle together the theory of equilibration in the weak coupling limit, it is important to understand just how large these instabilities and their associated magnetic fields grow. It has been of particular interest to understand the similarities and differences between the evolution of instabilities in non-abelian gauge theory plasmas vs. traditional abelian plasmas [8, 9, 11, 12].

As we'll briefly review, simulations have been previously devised to test whether non-abelian effects would limit the growth of plasma instabilities compared to abelian plasmas. An example of the results [8, 9] is shown in Fig. 1. This figure shows the growth in time of the magnetic energy of long-wavelength fields associated with the instability. In these simulations, the instability has been seeded with a very small initial amplitude. The dotted line shows the abelian case, corresponding to simple exponential growth of the instability (with a rate that can be computed in perturbation theory). This energy growth is fueled by stealing energy from the particles in the plasma, and it must eventually stop once the fraction of energy stolen becomes significant. In these simulations, that scale is beyond the top of the graph. (In fact, the back-reaction on the plasma particles is intentionally ignored in these simulations, providing an unlimited source of energy, so that one may cleanly disentangle whether or not non-abelian effects can limit the instability growth earlier.)

For computational simplicity, the first simulations of the non-abelian theory were restricted to one spatial dimension [7], in a specific sense reviewed later. From rough reasoning based on the one-dimensional theory, Ref. [6] had earlier conjectured that non-abelian interactions would not stop exponential growth of the instability. This conjecture was apparently supported by the one-dimensional simulations, an example of which is shown by the dashed line in Fig. 1. The growth starts out looking like the abelian case (which is expected from perturbative analysis of the instability). Eventually, there is a deviation when the fields get large enough for non-linear self-interactions in the non-abelian theory to become important, but the subsequently growth is again exponential. The conjecture proved wrong for the full three-dimensional theory, however, shown by the solid line in Fig. 1. After non-linear interactions become important, there is a spurt of rapid growth similar to the one-dimensional case, but then instability growth stops in three dimensions. There is continued linear growth in the magnetic energy at late times, shown in the linear plot of Fig. 1b, but this is due to the unstable modes pumping energy into slightly higher momentum, stable modes rather

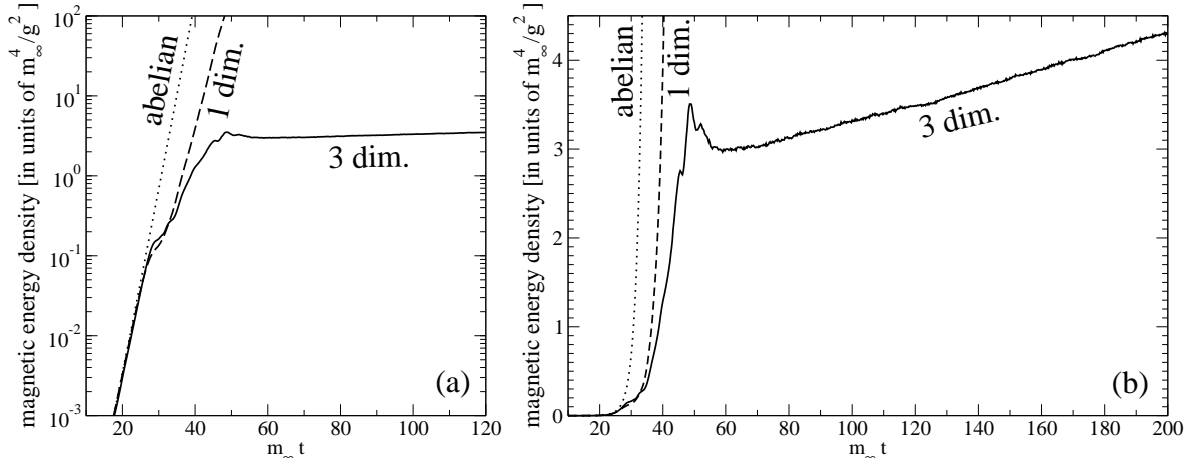


FIG. 1: The magnetic field energy associated with instabilities as a function of time for abelian theories (dotted line), non-abelian theories restricted to one spatial dimensions (dashed line), and non-abelian theories in three spatial dimensions (solid line). The vertical axis is shown as both (a) logarithmic, and (b) linear. These particular simulations are taken from Ref. [8], but similar one-dimensional simulations were performed earlier in Ref. [7]. The non-Abelian simulations are based on SU(2) gauge theory.

than by continued growth of the unstable modes [11].

The purpose of this paper is to investigate the root cause of the different behavior in one and three dimensions. Our tool will be the intermediate case of two dimensions. Before explaining our results, however, we need to review the three-dimensional theory being simulated and how one defines its reduction to lower dimensions. Following the review, we will present our two-dimensional results. We can get either one-dimensional or three-dimensional behavior, depending on how the two-dimensional theory is constructed. Then, in Sec. II, we offer a general interpretation of our results in terms of whether all polarizations of the gauge field are gauged in the dimensionally-reduced theory. For the sake of concreteness, we also discuss a specific example of this interpretation in the context of Nielsen-Olesen instabilities, which could possibly play a role in the fate of non-abelian plasma instabilities. Finally, we offer our conclusions in Sec. III. Technical details of our simulations are relegated to an appendix.

A. Review

Weibel instabilities occur when the momentum distribution of a non-equilibrium plasma is anisotropic, the expansion and collision rates are small compared to the instability growth rate, and there is a clear separation of scale between the momentum of typical plasma particles and the wave numbers associated with the resulting instability. The problem can be studied by simulating a non-abelian analog of the classical Vlasov equations of traditional plasma physics. In the weak coupling limit, one can justify the preceding assumptions and the application of these classical equations to the plasma instabilities in the bottom-up picture [2]. In the bottom-up picture, the energy stored in the plasma particles is parametrically larger than the energy associated with the onset of significant self-interactions of magnetic fields associated with the instability. The Vlasov equations consist of (i) a collisionless

Boltzmann equation describing the evolution of the phase space density $f(\mathbf{x}, \mathbf{p}, t)$ of hard quarks and gluons in the presence of a soft gauge field $A(\mathbf{x}, t)$, and (ii) Maxwell's equation for the soft gauge field with sources given by the hard particles. In order to study how large the instabilities grow, it is sufficient to linearize these equations in fluctuations $\delta f(\mathbf{x}, \mathbf{p}, t)$ of the hard particles about an initial (homogeneous) distribution $f_0(\mathbf{p})$, while retaining the non-linear structure of the non-abelian gauge field A . This approximation treats the plasma particles as an infinite reservoir of energy for instability growth. Schematically (suppressing sums over particles types), the equations are of the form¹

$$(D_t + \mathbf{v} \cdot \mathbf{D}_x) \delta f + g(\mathbf{E} + \mathbf{v} \times \mathbf{B}) \cdot \nabla_{\mathbf{p}} f_0 = 0, \quad (1.1a)$$

$$D_\nu F^{\mu\nu} = j^\mu = g\nu t_R \int \frac{d^3 p}{(2\pi)^3} v^\mu \delta f. \quad (1.1b)$$

Above, δf is in the adjoint representation, D is the corresponding covariant derivative, t_R is a group factor, ν counts particle spins and types,² and $v^\mu \equiv (1, \hat{\mathbf{p}})$. For ultra-relativistic systems, one can put these equations in a more convenient form by integrating over the magnitude $|\mathbf{p}|$ of momentum to replace $\delta f(\mathbf{x}, \mathbf{p})$, which depends on six phase-space coordinates, by a distribution $W(\mathbf{x}, \mathbf{v})$, which depends on only five since $\mathbf{v} = \hat{\mathbf{p}}$ lives on the unit sphere. $W^a(\mathbf{x}, \mathbf{v})$ represents the net adjoint color of all particles moving in direction \mathbf{v} at point \mathbf{x} . The corresponding Vlasov equations are

$$(D_t + \mathbf{v} \cdot \mathbf{D}_x) W + m_\infty^2 [\mathbf{E} \cdot (\nabla_{\mathbf{v}} - 2\mathbf{v}) - \mathbf{B} \cdot (\mathbf{v} \times \nabla_{\mathbf{v}})] \Omega(\mathbf{v}) = 0, \quad (1.2a)$$

$$D_\nu F^{\mu\nu} = j^\mu = \int_{\mathbf{v}} v^\mu W, \quad (1.2b)$$

where $\Omega(\mathbf{v})$ is determined by the angular dependence of the initial particle distribution $f_0(\mathbf{p})$, normalized so that the angular average of $\Omega(\mathbf{v})$ is one. The mass scale m_∞ above is set by the amplitude of f_0 as

$$m_\infty^2 \equiv g^2 \nu t_R \int_0^\infty \frac{d^3 p}{(2\pi)^3} \frac{f_0(p\mathbf{v})}{p}. \quad (1.3)$$

For moderately anisotropic plasmas, this is the order of magnitude of instability wavenumbers, instability growth rates, plasmon masses, and Debye screening, all of which we refer to as soft physics. Soft magnetic fields become non-perturbative when $B \sim m_\infty^2/g$, with corresponding energy density $\frac{1}{2}B^2 \sim m_\infty^4/g^2$.

In this paper, we focus on the case of moderately anisotropic, oblate velocity distributions which are axi-symmetric about the z axis. In particular, we will study precisely the same angular distribution $\Omega(\mathbf{v})$ studied in Ref. [8]. A full study of the bottom-up scenario will require simulating extremely anisotropic distributions [2, 14, 16], which is computationally more difficult. However, moderately anisotropic distributions will be adequate for the goal of this paper to understand the origin of the differences between one and three dimensional simulations. For the sake of numerical simplicity, our simulations are all based on SU(2) gauge theory rather than SU(3) QCD. We do not have any reason to expect qualitative differences between the two.

¹ We work in $(-+++)$ metric convention.

² For example, for a plasma of gluons, $\nu = 2$ and $t_R = 3$.

The “one dimensional” version of equations (1.1) and (1.2) consists of assuming that fields and distributions vary in space only in one direction z , as $A_\mu(z, t)$ and $\delta f(z, \mathbf{p}, t)$ [or $W(z, \mathbf{v}, t)$]. Particle momenta \mathbf{p} , however, are still treated three-dimensionally, and all three spatial polarizations of the gauge field (A_x, A_y, A_z) are included. This type of dimensional reduction of the full three dimensional theory is known in traditional plasma physics as a 1D+3V theory, where the 1D signifies that \mathbf{x} has been reduced to one dimension, but the 3V indicates that velocity (momentum) is still treated three-dimensionally. Fully three-dimensional simulations are 3D+3V. Note that if the transverse polarizations $A_x(z, t)$ and $A_y(z, t)$ were not included in one-dimensional simulations, one could not describe magnetic physics at all and so could not investigate Weibel instabilities.

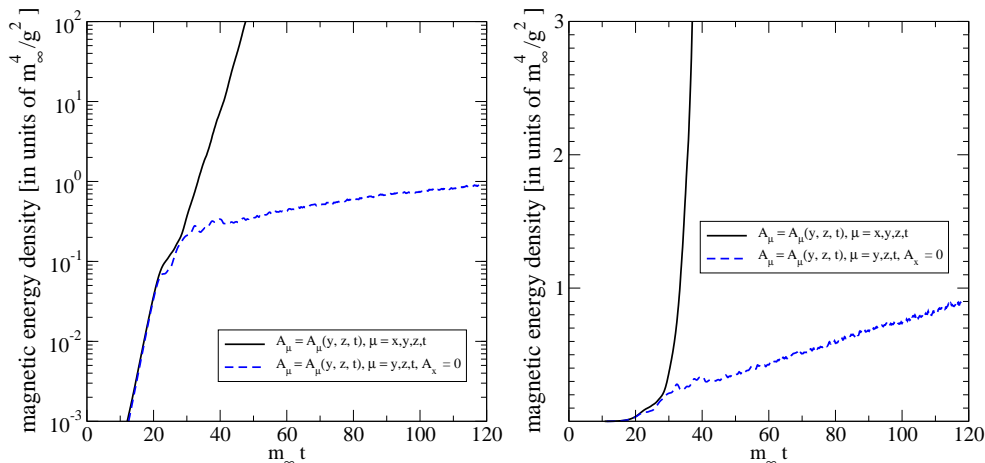
B. Two-Dimensional Results

Fig. 2 shows our results for two-dimensional (2D+3V) simulations. The solid line represents the same kind of dimensional reduction that was done in the one-dimensional case: all polarizations are retained, but fields and distributions depend on only two spatial dimensions:³

$$A_\mu = A_\mu(y, z, t), \quad \mu = x, y, z, t; \quad (1.4a)$$

$$\delta f = \delta f(y, z, \mathbf{p}, t), \quad (1.4b)$$

or $W = W(y, z, \mathbf{v}, t)$. [The labeling of directions with respect to the two-dimensional plane is shown in Fig. 3 for reference.] In this case, we find behavior similar to one-dimensional simulations: instability growth continues exponentially even after non-abelian interactions become important. However, the dashed line shows what happens if we eliminate the polarization A_x which lies outside of the two-dimensional plane, by setting $A_x = 0$ in our two-dimensional simulations. We now obtain behavior similar to three-dimensional simulations instead: the energy growth at late times is linear rather than exponential.



³ Though we have listed $\mu = t$ in (1.4a) for the sake of generality, the simulations are carried out in $A_0 = 0$ gauge. We will only discuss gauge-invariant results.

FIG. 2: As Fig. 1 but for two-dimensional (2D+3V) simulations. The solid line is for the straightforward dimensional reduction of (1.4). The dashed line is a simulation that does not include the out-of-plane polarization A_x .

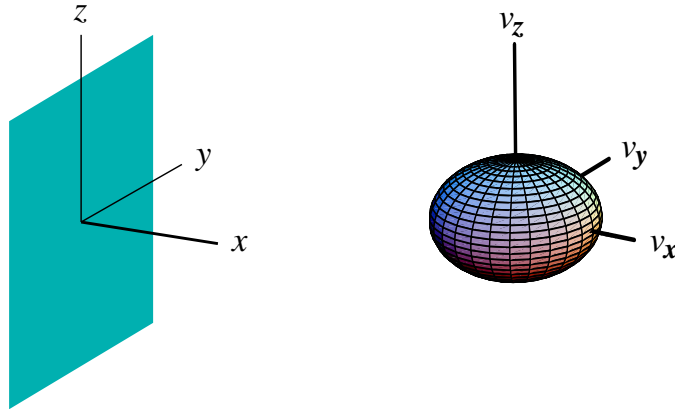


FIG. 3: Axis labeling for two-dimensional (2D+3V) simulations. The spatial plane \mathbf{x} is the yz plane, shown on the left, but particle momenta \mathbf{p} live in three dimensions, and the initial distribution $\Omega(\mathbf{v})$ of particle velocities is axi-symmetric about the z axis, as depicted on the right.

We can even produce both behaviors in one simulation, shown by the solid line in Fig. 4, by initializing the seed field for the out-of-plane component A_x much smaller than the other components. The solid line shows the total magnetic field energy, which, for times $m_\infty t \lesssim 80$, behaves similar to the $A_x = 0$ simulation shown by the dashed line of Fig. 2: initial exponential growth followed by linear growth. The dotted line in Fig. 4 shows the energy associated with A_x , which we take to be $\frac{1}{2}B_y^2 + \frac{1}{2}B_z^2 = \frac{1}{2}(D_y A_x)^2 + \frac{1}{2}(D_z A_x)^2$ in two dimensions. The importance of A_x continues to grow throughout. When it eventually catches up to the other components at $m_\infty t \simeq 100$, the linear behavior changes to the continued exponential growth we saw earlier in simulations where A_x was initialized on the same footing as the other components.

We have shown simulations that start from tiny initial seed fields for the instability. Similar results, shown in the Appendix, apply to two-dimensional simulations that start from large, non-perturbative initial configurations: the late-time growth of magnetic energy is exponential (like one-dimensional simulations) if the out-of-plane polarization A_x is included in the simulation, and linear (like three-dimensional simulations) if it is not.

II. INTERPRETATION

A. General

We can now offer a general characterization of what seems to determine whether non-abelian effects stop Weibel instability growth in 1D+3V, 2D+3V, and 3D+3V simulations (at least for the moderately anisotropic particle distribution we have simulated). Non-abelian effects will prevent late-time exponential growth if and only if no gauge-field polarizations are included outside of the subset of spatial dimensions simulated. In 1D, we have no choice; unless such polarizations are included, we cannot simulate magnetic fields and so

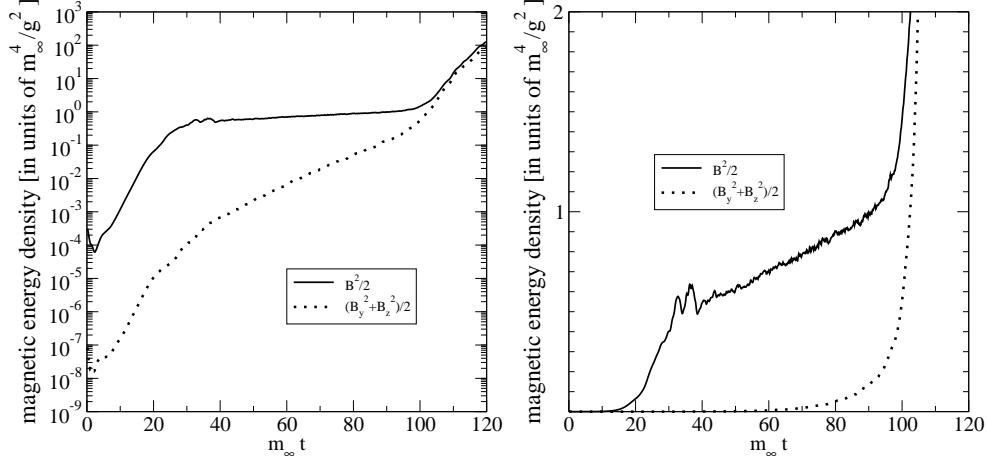


FIG. 4: As Fig. 2 but for a two-dimensional simulation with *very* small initial conditions for the out-of-plane polarization A_x . The solid line is the total magnetic energy $\frac{1}{2}B^2$; the dotted line is the energy density $\frac{1}{2}B_y^2 + \frac{1}{2}B_z^2$ associated with A_x .

cannot study the Weibel instability at all. In three dimensions, we automatically include all polarizations. In two dimensions, we have a choice, with the results described above.

Formally, the difference between gauge field polarizations in and out of the subset of spatial dimensions is that those within the subset (like A_y and A_z in two dimensions) are gauge fields in the dimensionally reduced theory, while those outside (like A_x) are instead adjoint-charge scalars. For the two-dimensional theory, for instance, the Yang-Mills Lagrangian is

$$\frac{1}{4}F_{\alpha\beta}^a F^{a\alpha\beta} + \frac{1}{2}(D_\alpha A_x)^a (D^\alpha A_x)^a, \quad (2.1)$$

where α and β are summed over the 2+1 dimensions (y, z, t). There is a significant difference between gauge fields and scalars. Gauge fields can always be locally transformed away so that $A = 0$ at any particular point, and scalars cannot. In our two-dimensional theory, the squared amplitude $A_x^a A_x^a$ of the two-dimensional scalar A_x is locally gauge invariant and can have physical consequences.

As an example, consider the two-dimensional theory, and imagine that a component of A has grown very large due to the instability. Let's focus on distance scales small compared to the wavelength of the unstable modes. As a first approximation, treat A as constant over these small distances and compare and contrast two situations: (i) a large, constant gauge component A_y or A_z , and (ii) a large, constant scalar component A_x . In the first case we can gauge away to $A_y = A_z = 0$, and so there is no effect at this order of approximation. One would have to start looking further to the derivatives of A (*i.e.* $F^{\mu\nu}$). In the second case, however, scalar background fields give rise to the Higgs mechanism. Except for adjoint color directions that commute with A_x , the gauge fields A_y and A_z will develop large masses of order gA_x . If A_x is large enough, this could plausibly suppress all fluctuations of the fields except in commuting color directions. If the unsuppressed fields all commute, then non-abelian interactions cannot prevent instability growth. This is equivalent to the “abelianization” conjecture of Ref. [6], which supposed that, once non-abelian interactions became important, their dynamics would approximately abelianize the fields and so allow for continued instability growth. What this conjecture did not appreciate was the difference between scalar fields, such as arise in the dimensionally reduced theory, and true gauge

fields.

To make this difference more concrete, we will now analyze a particular example of possible relevance to the physics of Weibel instabilities.

B. An Example: Nielsen-Olesen Instabilities

Three years ago, before any results had been obtained from three-dimensional simulations, Berndt Müller [18] suggested that three-dimensional instability growth would eventually have to stop because, even if the gauge fields did abelianize, Nielsen-Olesen instabilities [19] would eventually destroy nearly-abelian configurations as the fields continued to grow. In this section, we will briefly review these instabilities and discuss how they are suppressed if some components of gauge fields are replaced by scalar fields due to dimensional reduction.

For definiteness and simplicity, let us focus on $SU(2)$ gauge theory. Suppose that there is a large magnetic field whose color lies in an Abelian $U(1)$ subgroup. In our application, imagine that this is a large, abelianized magnetic field that might have formed due to the instability and non-abelian interactions. Over small enough distance and time scales (to be discussed later), we can approximate this magnetic field as constant. So, for instance,

$$B_i^a(\mathbf{x}, t) = \mathbf{B}_0 \delta^{a3}. \quad (2.2)$$

Now consider fluctuations about this background field. If we ignore the effects of the hard particles represented by $\delta f(\mathbf{x}, \mathbf{p}, t)$ in our application, but just consider pure Yang-Mills theory of the soft fields, then this is the problem studied by Nielsen and Olesen [19]. In general, the equation of motion for fluctuations a about a classical background A is

$$[D^2 g^{\mu\nu} - 2igF^{\mu\nu}]^{ab} a_\nu^b = 0 \quad (2.3)$$

if one works in background gauge ($D_\mu a^\mu = 0$) and if A satisfies the Yang-Mills equations of motion [which is the case for (2.2)]. Here $D = \partial - igA$ is the background covariant derivative in adjoint color representation. For the background (2.2), this equation can be decomposed into different sectors classified by (i) the color charge $Q = 0$ or ± 1 of a under the color generator T^3 and (ii) its spin projection $m_s = 0$ or ± 1 along the \mathbf{B}_0 axis. Eq. (2.3) becomes⁴

$$(D^2 + 2m_s QgB_0) a_{Qm_s} = 0 \quad (2.4)$$

where $D = \partial - iQgA$ is an Abelian background derivative with charge Qg . For $A_0 = 0$, Fourier transforming t to ω gives

$$[-(\nabla - iQg\mathbf{A})^2 - 2m_s QgB_0] a_{Qm} = \omega^2 a_{Qm_s}. \quad (2.5)$$

Mathematically, this is a relativistic generalization of the Schrödinger equation for a particle with spin in a constant magnetic field. It has precisely the form of the non-relativistic Schrödinger equation with the non-relativistic energy E replaced by $\omega^2/2M$. The $2m_s QgB_0$ term represents the effect on the energy of the interaction between the gluon spin and

⁴ Specifically, $a^{ai}(x) = \sum_{Q, m_s} a_{Q, m_s}(x) \zeta_Q^a \zeta_{m_s}^i$, where Q and m_s run over 0 and ± 1 ; $\zeta_{\pm 1} = \xi_{\pm 1} = (1, \pm i, 0)$, $\zeta_0 = \xi_0 = (0, 0, 1)$; and $a_{-Q, -m_s} = a_{Q, m_s}^*$.

the magnetic field. The values of ω^2 are determined by (2.5) to be the eigenvalues of the Hamiltonian

$$H_{Q,m_s} = (\mathbf{p} - Qg\mathbf{A})^2 - 2m_s QgB_0. \quad (2.6)$$

For the three-dimensional case, one may now follow the discussion of Landau levels in any quantum mechanics textbook. The eigenvalues are

$$\omega^2 = p_{\parallel}^2 + (n + \frac{1}{2})2gB_0 - 2m_s QgB_0. \quad (2.7)$$

The first term is from the component p_{\parallel} of momentum parallel to the magnetic field \mathbf{B}_0 , the second is the Landau level energy in the plane orthogonal to \mathbf{B}_0 , and the last is the spin interaction with \mathbf{B}_0 . The interesting case here is $Q = m_s = \pm 1$, for which the lowest Landau orbital gives

$$\omega^2 = p_{\parallel}^2 - gB_0, \quad (2.8)$$

which is negative for $p_{\parallel} \leq (gB_0)^{1/2}$. There are therefore unstable modes in the relativistic, classical field theory problem.⁵ This is the Nielsen-Olesen instability. Since it produces growth of gauge field fluctuations a with non-trivial T^3 charge—that is, of colors which do not commute with the original field A —it is an instability which will tend to destroy abelianization of the gauge fields.

But now let's consider the same Hamiltonian (2.6) for the dimensionally-reduced theory. For example, $p_x = 0$ in a two dimensional theory of the yz plane, and so (focusing on the previously unstable case $Q = m_s = \pm 1$):

$$H_{\pm 1, \pm 1} = (gA_x)^2 + (p_y \mp gA_y)^2 + (p_z \mp gA_z)^2 - 2gB_0. \quad (2.9)$$

This Hamiltonian is bounded below by $(gA_x)^2 - 2gB_0$. If the A_x field is large enough that

$$(gA_x)^2 > 2gB_0, \quad (2.10)$$

then there will be no negative eigenvalue and so no Nielsen-Olesen instability. In fact, the $(gA_x)^2$ contribution to the relation that determines ω^2 is just the Higgs mechanism due to a background scalar field A_x , as discussed earlier.

The one-dimensional case is similar, with now

$$H_{\pm 1, \pm 1} = (gA_x)^2 + (gA_y)^2 + (p_z \mp gA_z)^2 - 2gB_0 \quad (2.11)$$

bounded below by $(gA_x)^2 + (gA_y)^2 - 2gB_0$.

We can usefully recast some of our conditions for the application to Weibel instability growth. By treating the magnetic field as constant, we found Nielsen-Olesen instabilities in three dimensions with typical moment $p_{\parallel} \sim (gB)^{1/2}$ and growth rates $\Gamma = (-\omega^2)^{1/2} \sim (gB)^{1/2}$. The constant magnetic field approximation will be okay if these scales are large compared to the typical momentum scale k of B . So we need $(gB)^{1/2} \gg k$, which is

$$B \gg \frac{k^2}{g}. \quad (2.12)$$

⁵ Note that there is nothing unstable in the non-relativistic Schrödinger problem. The instability $\omega^2 < 0$ in the relativistic, classical field theory problem simply corresponds to a negative energy state in the corresponding non-relativistic Schrödinger problem.

This is simply the condition for the field to have grown past the point where non-Abelian interactions become important.

For the two-dimensional theory, we can recast condition (2.10) for suppressing Nielsen-Olesen instabilities into a similar form. Using $B_y = D_z A_x \sim k A_x$, the condition is

$$B \gtrsim \frac{k^2}{g} \left(\frac{B}{B_y} \right)^2. \quad (2.13)$$

So, unless B_y is an unusually small component of the magnetic field (because we set $A_x = 0$, for example), then the Nielsen-Olesen instability will be suppressed in the dimensionally reduced theory just when it first might have become important, as determined by (2.12).

III. CONCLUSIONS

It is sometimes desirable to simplify a theory, such as through dimensional reduction, in order to reduce the cost of numerical simulations. For studying the fate of non-abelian Weibel instabilities, we have found qualitatively different behavior in lower-dimensional simulations when polarizations A of the gauge field are included that are not gauge fields in the lower-dimensional theory. This rules out using one-dimensional (1D+3V) simulations to investigate the fate of non-abelian Weibel instabilities. However, two-dimensional (2D+3V) simulations can be made to behave similar to the three-dimensional case if the out-of-plane polarization of A is discarded. So far, we have not investigated the case of extremely anisotropic distributions.

Acknowledgments

We are deeply indebted to Guy D. Moore for providing the original 3-dimensional simulation code that was adapted for this project. We thank Berndt Müller for several conversations over the past few years related to Nielsen-Olesen instabilities. This work was supported, in part, by the U.S. Department of Energy under Grant No. DE-FG02-97ER41027.

APPENDIX A: SIMULATION DETAILS

1. Basics

We use the same simulation method as Ref. [8], discretizing dependence of $W(\mathbf{x}, \mathbf{v}, t)$ on velocity \mathbf{v} in terms of spherical harmonics $Y_{lm}(\mathbf{v})$ for $m \leq l \leq l_{\max}$. For our initial conditions, we choose a seed magnetic field configuration and start with zero electric field and hard particle fluctuation W . For simulations with small initial conditions, the initial magnetic field was chosen such that the gauge fields A have a Gaussian distribution with an exponential fall-off in \mathbf{k} as in Ref. [8]. Our canonical choice of parameters for two-dimensional simulations was lattice spacing $a = 0.125/m_\infty$ on a 256×256 lattice of physical size $L^2 = (256a)^2 = (32/m_\infty)^2$, and $l_{\max} = 12$ with damping on large l as in Ref. [11].

A relatively simple way to simulate the out-of-plane polarization A_x in our 2D+3V simulations is to simply run 3D+3V simulations on $1 \times N_y \times N_z$ lattices. The links U_x in the short periodic direction of size $N_x = 1$ encode the physics of $A_x(y, z, t)$. However, we found

it simpler to adapt three-dimensional simulations by instead simulating $2 \times N_y \times N_z$ lattices with initial conditions that are translation invariant in the short direction $N_x = 2$. The reason is that the procedure for updating the W field, as described in Sec. V B and V D of Ref. [20], involves alternating updating W on only the even spatial sub-lattice on one time step and only the odd spatial sub-lattice the next time step. For each update of W at a site, the algorithm assumes that W at neighboring sites is fixed. That assumption would fail for a $1 \times N_y \times N_z$ lattice because every site is its own neighbor.⁶

2. Initial conditions

The simulations discussed in the main text all started with tiny seeds for the unstable modes. They all have initial exponential growth, as predicted by a perturbative analysis of the instability. In Ref. [11], it was noted that linear energy growth sets in immediately in three-dimensional simulations if one instead starts with non-perturbatively large seeds for the unstable modes. To check the robustness of our conclusions, we have made similar simulations in two dimensions. The results are shown in Fig. 5 and 6. As with the case of small initial conditions, the late-time behavior is exponential if A_x is included and linear if not.

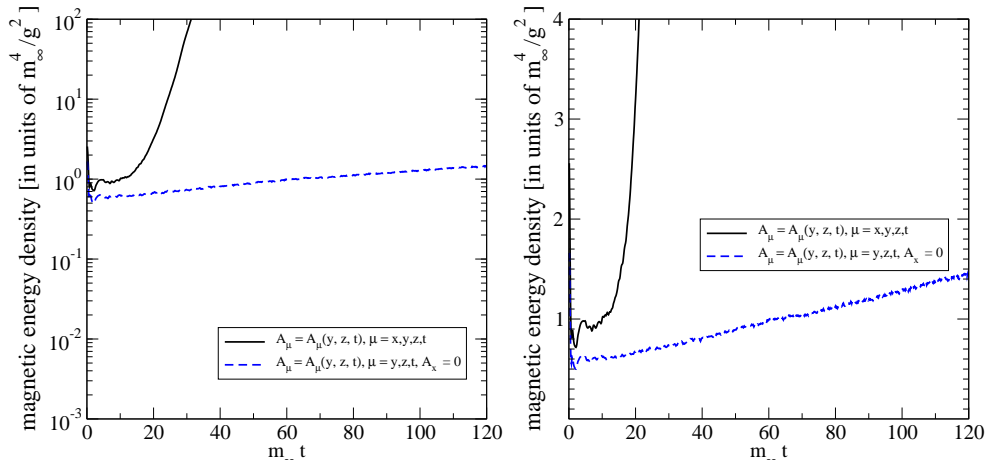


FIG. 5: As Fig. 2 but for two-dimensional simulations with large initial conditions. The initial condition is selected from a thermal ensemble with temperature $T = 2m_\infty/g^2$, which is then gauge-invariantly smeared to remove high-momentum components, exactly as in Ref. [11]. [As in Ref. [11], the amount of smearing was chosen so that perturbatively it would correspond to multiplying the thermal spectrum for $A(\mathbf{k})$ by $\exp(-k^2/4m_\infty^2)$.] For the $A_x = 0$ simulation, the links U in the x direction are then set to unity.

⁶ Ignoring this issue and proceeding with a periodic lattice with $N_x = 1$ introduces artificial numerical instabilities unless one modifies the W update algorithm. This numerical instability can be understood analytically by considering a free W field ($\partial_t W + \mathbf{v} \cdot \nabla W = 0$), finding the corresponding discrete-time lattice dispersion relation for a given algorithm, and checking whether the solution for the frequency ω ever produces a positive imaginary part.

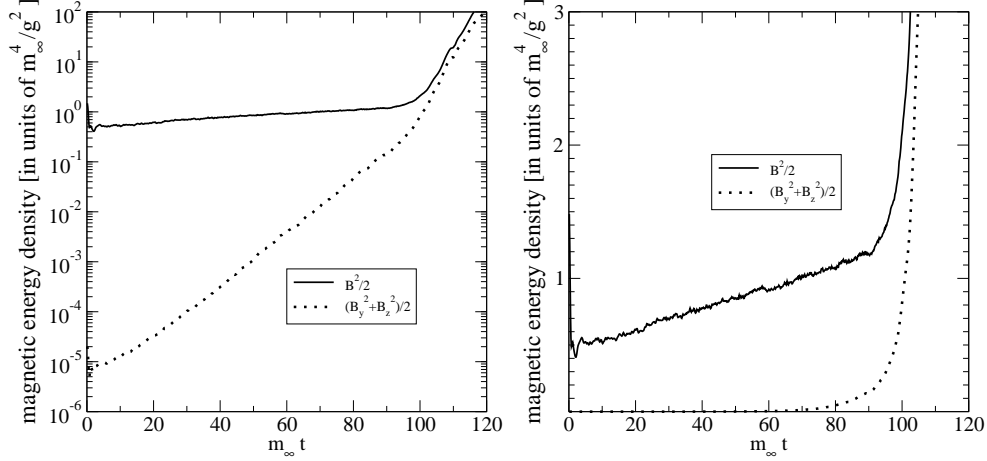


FIG. 6: As Fig. 4 but the initial conditions for the 2-dimensional gauge fields A_y and A_z are large, while the out-of-plane component A_x is initialized small.

3. Systematic errors

Ref. [8] provides many checks that their three-dimensional simulation results are not significantly affected by discretization effects. Because the canonical simulation parameters we use for two-dimensional simulations in this paper are as good or better than the canonical parameters of Ref. [8], one might expect that there are no significant discretization effects. To be thorough, however, we present studies of lattice spacing dependence, volume dependence, and l_{\max} dependence in Figs. 7–10. We show here results for simulations with large, non-perturbative initial conditions, such as discussed above; results are similar for small initial conditions.

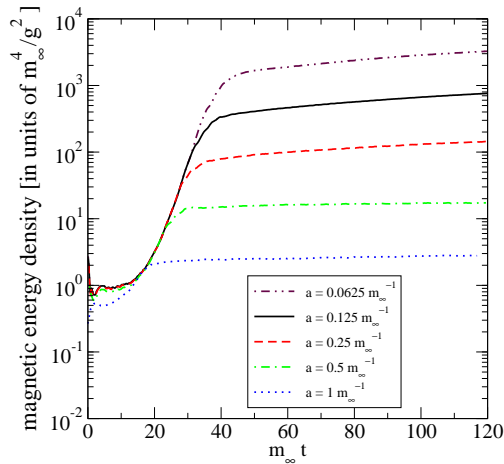


FIG. 7: Magnetic energy vs. time showing results for several different choices of lattice spacing for a volume $L^2 = (32/m_\infty)^2$ with all polarizations retained (i.e. including A_x).

The curves in Fig. 7 are like the solid line in left-hand plot of Fig. 5, where we saw continued exponential growth, except that here we show explicitly what happens when the fields get so large that they become limited by the effects of the discrete lattice. The proof

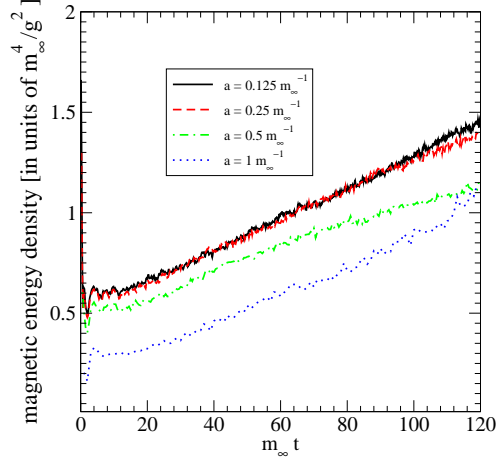


FIG. 8: Linear plot of Magnetic energy vs. time showing results for several different choices of lattice spacing for a volume $L^2 = (32/m_\infty)^2$ with out-of-plane polarization A_x not included.

that this limit is a lattice artifact is that it increase steadily as the lattice spacing is reduced, as seen in Fig. 7. In contrast, the curves in Fig. 8 show the case $A_x = 0$. These curves are like the dashed line in the right-hand plot of Fig. 5, where we saw late-time linear energy growth. We see here that this behavior is robust as we decrease the lattice spacing, and that $a = 0.25/m_\infty$ is an adequately small spacing for our simulations.

Fig. 9 shows an example of dependence on physical two-dimensional volume L^2 for the case of continued exponential growth. (The apparent end to exponential growth shown in this figure is the same finite-spacing lattice artifact seen in Fig. 7. We see that nothing changes qualitatively as the volume is increased: the exponential growth beyond the non-perturbative scale remains. In examining the quantitative variation between the curves, one should keep in mind that it is not possible to use the same initial conditions for simulations with different volume: in addition to systematic effects, there is statistical variation reflecting the random choice of initial conditions.

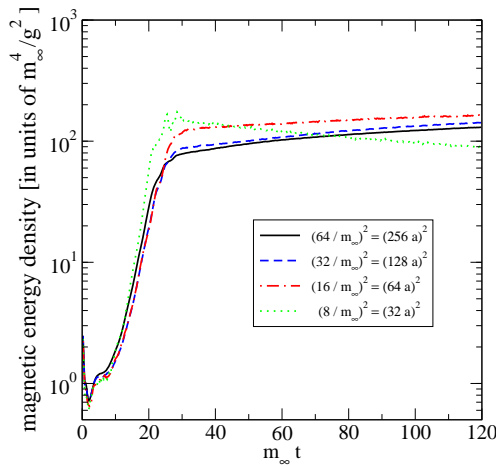


FIG. 9: Magnetic energy vs. time showing results for several different physical volumes with lattice spacing $a = 0.25/m_\infty$. A_x is included in these simulations.

Finally, Fig. 10 is the analogous figure for l_{\max} dependence. We see that $l_{\max} = 12$ is an

adequate approximation to the large l_{\max} limit for our simulations.

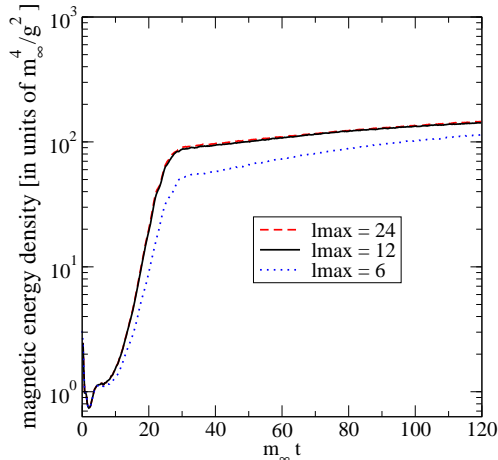


FIG. 10: Magnetic energy vs. time showing results for several different choices of l_{\max} with $a = 0.25/m_\infty$ and $L^2 = (32/m_\infty)^2$. A_x is included in these simulations.

-
- [1] R. Baier, A. H. Mueller, D. Schiff and D. T. Son, “‘Bottom-up’ thermalization in heavy ion collisions,” *Phys. Lett. B* **502**, 51 (2001) [hep-ph/0009237].
 - [2] P. Arnold, J. Lenaghan and G. D. Moore, “QCD plasma instabilities and bottom-up thermalization,” *JHEP* 08 (2003) 002 [hep-ph/0307325].
 - [3] E. S. Weibel, “Spontaneously growing transverse waves in a plasma due to an anisotropic velocity distribution,” *Phys. Rev. Lett.* **2**, 83 (1959).
 - [4] S. Mrówczyński, “Stream instabilities of the quark-gluon plasma,” *Phys. Lett. B* **214**, 587 (1988); Y. E. Pokrovsky and A. V. Selikhov, “Filamentation in a quark-gluon plasma,” *JETP Lett.* **47**, 12 (1988) [*Pisma Zh. Eksp. Teor. Fiz.* **47**, 11 (1988)]; “Filamentation in quark plasma at finite temperatures,” *Sov. J. Nucl. Phys.* **52**, 146 (1990) [*Yad. Fiz.* **52**, 229 (1990)]; “Filamentation in the quark-gluon plasma at finite temperatures,” *Sov. J. Nucl. Phys.* **52**, 385 (1990) [*Yad. Fiz.* **52**, 605 (1990)]; O. P. Pavlenko, “Filamentation instability of hot quark-gluon plasma with hard jet,” *Sov. J. Nucl. Phys.* **55**, 1243 (1992) [*Yad. Fiz.* **55**, 2239 (1992)]; S. Mrówczyński, “Plasma instability at the initial stage of ultrarelativistic heavy ion collisions,” *Phys. Lett. B* **314**, 118 (1993); “Color collective effects at the early stage of ultrarelativistic heavy ion collisions,” *Phys. Rev. C* **49**, 2191 (1994); “Color filamentation in ultrarelativistic heavy-ion collisions,” *Phys. Lett. B* **393**, 26 (1997) [hep-ph/9606442].
 - [5] P. Romatschke and M. Strickland, “Collective modes of an anisotropic quark gluon plasma,” *Phys. Rev. D* **68**, 036004 (2003) [hep-ph/0304092].
 - [6] P. Arnold and J. Lenaghan, “The abelianization of QCD plasma instabilities,” *Phys. Rev. D* **70**, 114007 (2004) [hep-ph/0408052].
 - [7] A. Rebhan, P. Romatschke and M. Strickland, “Hard-loop dynamics of non-Abelian plasma instabilities,” *Phys. Rev. Lett.* **94**, 102303 (2005) [hep-ph/0412016].
 - [8] P. Arnold, G. D. Moore and L. G. Yaffe, “The fate of non-abelian plasma instabilities in 3+1 dimensions,” *Phys. Rev. D* **72**, 054003 (2005) [hep-ph/0505212].

- [9] A. Rebhan, P. Romatschke and M. Strickland, “Dynamics of quark-gluon plasma instabilities in discretized hard-loop approximation,” *JHEP* 09 (2005) 041 [hep-ph/0505261].
- [10] A. Dumitru and Y. Nara, “QCD plasma instabilities and isotropization,” *Phys. Lett. B* **621**, 89 (2005) [hep-ph/0503121].
- [11] P. Arnold and G. D. Moore, “QCD plasma instabilities: The nonabelian cascade,” *Phys. Rev. D* **73**, 025006 (2006) [hep-ph/0509206].
- [12] A. Dumitru, Y. Nara and M. Strickland, “Ultraviolet avalanche in anisotropic non-Abelian plasmas,” *Phys. Rev. D* **75**, 025016 (2007) [hep-ph/0604149].
- [13] P. Romatschke and R. Venugopalan, “Collective non-Abelian instabilities in a melting color glass condensate,” *Phys. Rev. Lett.* **96**, 062302 (2006) [hep-ph/0510121]; “The unstable Glasma,” *Phys. Rev. D* **74**, 045011 (2006) [hep-ph/0605045].
- [14] P. Arnold and G. D. Moore, “The turbulent spectrum created by non-Abelian plasma instabilities,” *Phys. Rev. D* **73**, 025013 (2006) [hep-ph/0509226].
- [15] A. H. Mueller, A. I. Shoshi and S. M. H. Wong, “A possible modified ‘bottom-up’ thermalization in heavy ion collisions,” hep-ph/0505164.
- [16] D. Bödeker, “The impact of QCD plasma instabilities on bottom-up thermalization,” hep-ph/0508223.
- [17] A. H. Mueller, A. I. Shoshi and S. M. H. Wong, “On Kolmogorov wave turbulence in QCD,” *Nucl. Phys. B* **760**, 145 (2007) [hep-ph/0607136].
- [18] Berndt Müller, private communication (2004).
- [19] N. K. Nielsen and P. Olesen, “An Unstable Yang-Mills Field Mode,” *Nucl. Phys. B* **144**, 376 (1978).
- [20] D. Bödeker, G. D. Moore and K. Rummukainen, “Chern-Simons number diffusion and hard thermal loops on the lattice,” *Phys. Rev. D* **61**, 056003 (2000) [hep-ph/9907545].